Tensor and complex anchoring in liquid crystals

S. V. Shiyanovskii,[1,2] A. Glushchenko,[3] Yu. Reznikov,[1,3] O. D. Lavrentovich,[1] and J. L. West[1]
[1]*Liquid Crystal Institute, Kent State University, Kent, Ohio 44242*
[2]*Institute for Nuclear Research, 47 Prospect Nauki, Kyiv, 03039, Ukraine*
[3]*Institute of Physics, 46 Prospect Nauki, Kyiv, 03039, Ukraine*
(Received 1 March 2000)

We propose a tensor description of surface anchoring of liquid crystals (LCs). The model allows one to consider both the homogeneous and inhomogeneous parts of LC anchoring and to calculate the cumulative effect of different treatments as a sum of corresponding tensors. For the planar alignment the tensor representation is reduced to the complex azimuthal anchoring coefficient, whose amplitude and phase determine, respectively, the strength of azimuthal anchoring and the azimuthal angle of the easy axis. We predict and experimentally confirm that two consecutive photoalignment treatments with beams of perpendicular polarizations can compensate each other and restore the initial anchoring.

PACS number(s): 61.30.−v, 68.10.Cr

Until the 1990s, the only practical technique to align liquid crystals (LCs) was to establish a fixed anchoring direction before the LC cell was assembled; for example, by depositing SiO_x or by buffing a polymer layer. Once assembled, the cells preserved the anchoring characteristics. The situation has been changed by the discovery of photoalignment techniques that allow one to align and realign the director $\hat{\mathbf{n}}$ on the substrate of a filled cell [1,2]. This progress calls for a new model of anchoring, capable of predicting the cumulative effect of subsequent alignment treatments, such as the appearance of a macroscopic alignment on an amorphous or polycrystalline substrate after polarized light irradiation.

The traditional description of LC anchoring operates with the axis of easy director orientation $\hat{\mathbf{e}}$ and the anchoring energy W that characterizes the work required to deviate $\hat{\mathbf{n}}$ from the easy axis. Deviations from the easy axis in the polar and azimuthal planes are characterized by two scalar coefficients W_p and W_a, respectively. This model is not well suited to describe the processes of alignment and realignment, when all the relevant quantities such as the easy axis, W_p and W_a change.

In this Rapid Communication we propose a tensor phenomenological description of surface anchoring in LCs by presenting the surface energy per unit area as

$$f_s = -\frac{1}{2}\sum_{\alpha,\beta} W_{\alpha\beta}(\mathbf{r}) n_\alpha n_\beta, \tag{1}$$

where $W_{\alpha\beta}(\mathbf{r})$ is the traceless symmetrical local anchoring tensor. The tensor approach allows us to consider both the homogeneous and inhomogeneous parts of anchoring and offers a natural way of handling the problems listed above. We illustrate the proposed approach experimentally.

Tensor approach

To derive Eq. (1), we refer to the model of a polymer alignment layer, with the Maier-Saupe pair interaction between LC molecules and polymer fragments. Under the assumption that the polymer alignment does not disturb the surface scalar order parameter S_b, f_s reads

$$f_s = f_{is}[(\hat{\mathbf{n}}\cdot\hat{\mathbf{k}})^2] - \frac{1}{\sigma}\sum_i \sum_{j\in\sigma} w(\mathbf{r}_i - \mathbf{r}_j) P_2(\hat{\mathbf{m}}_i\cdot\hat{\mathbf{l}}_j), \tag{2}$$

where $\Sigma_{j\in\sigma}$ is a sum over polymer fragments inside the small area σ, P_2 denotes the second order Legendre polynomial, $\hat{\mathbf{m}}_i$ (or $\hat{\mathbf{l}}_j$) defines orientation of the long axis of the ith LC molecule (or the jth polymer fragment) positioned at $\mathbf{r}_i$ (or $\mathbf{r}_j$), and $w(\mathbf{r}_i - \mathbf{r}_j)$ is the potential of the anisotropic interaction between the LC molecule and the polymer fragment. f_{is} is the surface energy density on the surface with isotropically distributed polymer fragments, which is an even function of the product of $\hat{\mathbf{n}}$ and the unit surface normal $\hat{\mathbf{k}}$ [3]. Far from the anchoring transition $f_{is} \approx B_0 + B_1(\hat{\mathbf{n}}\cdot\hat{\mathbf{k}})^2$ (B_0 and B_1 are constants) and averaging over orientations of LC molecules one obtains Eq. (1). For a short-range potential $w(\mathbf{r}_i - \mathbf{r}_j)$, $W_{\alpha\beta}(\mathbf{r})$ is represented as

$$W_{\alpha\beta}(\mathbf{r}) = \overline{W} S_b L_{\alpha\beta}(\mathbf{r}) - 2B_1\left(k_\alpha k_\beta - \frac{1}{3}\delta_{\alpha\beta}\right). \tag{3}$$

Here $\overline{W} = \frac{2}{\sigma}\Sigma_i \Sigma_{j\in\sigma} w(\mathbf{r}_i - \mathbf{r}_j)$, and $L_{\alpha\beta}(\mathbf{r}) = \langle l_j^\alpha(\mathbf{r}) l_j^\beta(\mathbf{r})\rangle - \frac{1}{3}\delta_{\alpha\beta}$ is the local tensor order parameter of the polymer fragments. Minimum of the surface energy (1) can be easily found in the eigen frame $\{\hat{\mathbf{e}}_j\}$ (j=1,2,3), where $W_{\alpha\beta}(\mathbf{r})$ is diagonal with eigenvalues $W_1 > W_2, W_3$. In the frame $\{\hat{\mathbf{e}}_j\}$, which is orthogonal due to the symmetry $W_{\alpha\beta}(\mathbf{r}) = W_{\beta\alpha}(\mathbf{r})$, Eq. (1) reads

$$f_s = -\frac{W_1}{2} + \frac{W_1 - W_2}{2} n_2^2 + \frac{W_1 - W_3}{2} n_3^2, \tag{4}$$

where n_j are the director components in this frame. The second and the third terms in Eq. (4) are non-negative, so that the axis $\hat{\mathbf{e}}_1$, which corresponds to the maximum eigenvalue W_1, is exactly the easy axis, while the quantities (W_1

$-W_2$) and (W_1-W_3) determine the traditional azimuthal and polar anchoring coefficients.

A comparison of Eq. (1) and Eq. (4) shows the difference between the tensor and the traditional approaches. The traditional description is equivalent to the tensor one in the eigenframe $\{\hat{\mathbf{e}}_j\}$. This frame rotates from point to point and during a treatment, making the description cumbersome. The tensor description has the covariant form and thus describes random anchoring and consecutive treatments in any reference frame.

One has to distinguish the local $W_{\alpha\beta}(\mathbf{r})$ and its macroscopic average over the whole surface $\langle W_{\alpha\beta}(\mathbf{r})\rangle_{\mathbf{r}}$. An untreated inhomogeneous substrate has macroscopic azimuthal symmetry, therefore, the average polymer tensor order parameter $\langle L^{in}_{\alpha\beta}(\mathbf{r})\rangle_{\mathbf{r}}$ should be diagonal in the $0xyz$ frame $(0z\|\hat{\mathbf{k}})$ with diagonal elements $\langle L^{in}_{xx}(\mathbf{r})\rangle_{\mathbf{r}}=\langle L^{in}_{yy}(\mathbf{r})\rangle_{\mathbf{r}}=L_{||}$ and $\langle L^{in}_{zz}(\mathbf{r})\rangle_{\mathbf{r}}=L_{\perp}$. According to Eq. (3), the average anchoring tensor $\langle W^{in}_{\alpha\beta}(\mathbf{r})\rangle_{\mathbf{r}}$ should have the same form $\langle W^{in}_{xx}(\mathbf{r})\rangle_{\mathbf{r}}=\langle W^{in}_{yy}(\mathbf{r})\rangle_{\mathbf{r}}=W_{||}$ and $\langle W^{in}_{zz}(\mathbf{r})\rangle_{\mathbf{r}}=W_{\perp}$. Since the two diagonal elements are equal, orientation of the easy axis is degenerate (the only exception is strictly normal orientation). Therefore, even a small deviation of $W^{in}_{\alpha\beta}(\mathbf{r})$ from $\langle W^{in}_{\alpha\beta}(\mathbf{r})\rangle_{\mathbf{r}}$, caused by local inhomogeneities in orientation of aligning fragments, lifts the degeneracy and sets a unique orientation of the local easy axis.

Photoalignment on polymer surface leads to additional orientational ordering of the aligning fragments. If the initial local variations of the polymer order are small, $|L^{in}_{\alpha\beta}(\mathbf{r})-\langle L^{in}_{\alpha\beta}(\mathbf{r})\rangle_{\mathbf{r}}|\ll 1$, the additional order $L^{k}_{\alpha\beta}(\mathbf{r})$, caused by the kth uniform treatment, does not depend on these variations and is also uniform: $L^{k}_{\alpha\beta}(\mathbf{r})=\langle L^{k}_{\alpha\beta}(\mathbf{r})\rangle_{\mathbf{r}}=L^{k}_{\alpha\beta}$. Thus, the ''weak'' treatments, which affect only a small fraction of the polymer fragments, lead to the final anchoring tensor W that is simply a sum of the random initial anchoring W^{in} and the contributions $\mathsf{W}^{(k)}$ of different treatments:

$$\mathsf{W}(\mathbf{r})=\mathsf{W}^{in}(\mathbf{r})+\sum_k \mathsf{W}^{(k)}, \tag{5}$$

where $\mathsf{W}^{(k)}$ is diagonal in the frame which corresponds to the induced easy axis $\hat{\mathbf{e}}^{(k)}$. The effect of ''strong'' treatments, which reorient a substantial fraction of the polymer fragments, can also be expressed with Eq. (5), but in this case $\mathsf{W}^{(k)}$ are nonlinear functions of the irradiation times τ_k and the sequence of the different treatments is crucial.

It should be noted that Eq. (5) is not suitable to describe photoalignment on dynamically equilibrium substrates (such as Langmuir-Blodgett films). In this case photoinduced reorientation of entire domains was observed and was described by the macroscopic model [4].

Complex representation for planar anchoring

Substantial simplification can be achieved for the tangential (in-plane) alignment that corresponds to $W_{yz}=W_{xz}=0$. It is useful to specify the director on a complex plane: $\tilde{n}=n_x+in_y=\cos\theta e^{i\varphi}$, where θ is a polar angle and φ is the azimuthal angle. The surface energy (1) takes the form

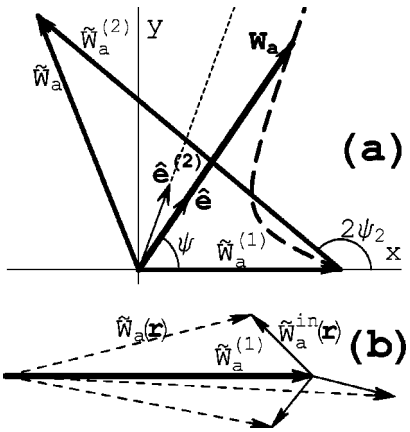

FIG. 1. Graphic representation of the complex anchorings [Eq. (7)]. (a) The cumulative effect of two homogeneous treatments with different induced easy axes: $\hat{\mathbf{e}}^{(1)}\|0x$ and $\hat{\mathbf{e}}^{(2)}$ making the angle ψ_2 with $0x$ axis; dashed curve shows the trajectory of the vector $\mathbf{W}_a=W_a\hat{\mathbf{e}}$ when $W_a^{(2)}$ increases. (b) The effect of the unidirectional homogeneous treatment $\tilde{W}_a^1$ (thick arrow) at different points of an inhomogeneous substrate with local anchorings $\tilde{W}_a^{in}(\mathbf{r})$ (thin arrows); $\tilde{W}_a(\mathbf{r})$ (dashed arrows) are the resulting anchorings at the same points of the surface.

$$f_s=f_{s0}-\frac{1}{8}(\tilde{W}_a^*\tilde{n}\tilde{n}+\tilde{W}_a\tilde{n}^*\tilde{n}^*)+\frac{3}{4}W_{zz}\tilde{n}\tilde{n}^*$$

$$=f'_{s0}+\frac{1}{2}W_a\cos^2\theta\sin^2(\varphi-\psi)+\frac{1}{2}W_p\sin^2\theta, \tag{6}$$

where f_{s0} and f'_{s0} are insignificant constants, which may be dropped, $\tilde{W}_a=W_{xx}-W_{yy}+2iW_{xy}=W_ae^{i2\psi}$ is the complex azimuthal anchoring coefficient, and $W_p=\frac{1}{2}(W_a-3W_{zz})$. The complex representation has the following advantages:

(1) W_p, W_a, and ψ in Eq. (6) and in the definition $\tilde{W}_a=W_ae^{i2\psi}$ are simply the traditional anchoring coefficients and the azimuthal angle of the easy axis, respectively.

(2) W_a is the linear combination of tensor components, thus the complex representation preserves the additivity of different treatments:

$$\tilde{W}_a(\mathbf{r})=\tilde{W}_a^{in}(\mathbf{r})+\sum_k \tilde{W}_a^{(k)}. \tag{7}$$

(3) Any treatment is presented in a compact form $\tilde{W}_a^{(k)}=W_a^{(k)}\exp(2i\psi_k)$, where the phase describes the orientation ψ_k of the induced easy axis and the amplitude $W_a^{(k)}$ corresponds to the strength of the treatment. One can visualize different surface treatments graphically presenting $\tilde{W}_a^{(k)}$ by vectors in the complex plane; see Fig. 1.

We illustrate the complex representation by the following examples. A substrate with a uniform in-plane easy axis is irradiated with polarized light that produces a different easy axis. According to Eq. (7) the resulting complex anchoring $\tilde{W}_a$ is the sum of the initial anchoring $\tilde{W}_a^{(1)}=W_a^{(1)}\exp(2i\psi_1)$ and light-induced anchoring $\tilde{W}_a^{(2)}=W_a^{(2)}\exp(2i\psi_2)$. The amplitude $W_a^{(2)}$ is controlled by the exposure. When the initial and the light-favored easy axes are not perpendicular, the

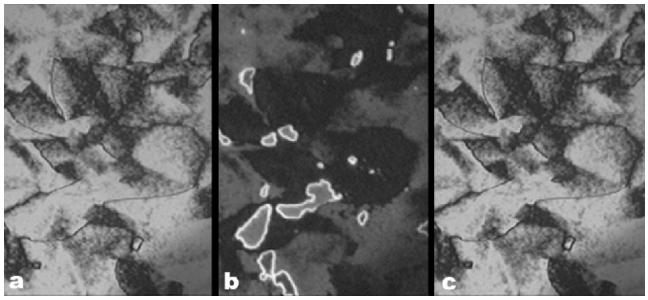

FIG. 2. The textures of the same spot (about 250 μm wide) before irradiation (a), after the first irradiation with $\hat{\mathbf{e}}_{uv}^{(1)} \perp \hat{\mathbf{e}}_{rub}$, $\tau_1 = 15$ s (b), and after the second irradiation with $\hat{\mathbf{e}}_{uv}^{(2)} \| \hat{\mathbf{e}}_{rub}$, $\tau_2 = 45$ s (c). Parallel polarizers.

increase of $W_a^{(2)}$ leads to a continuous rotation of the easy axis $\hat{\mathbf{e}}$ from ψ_1 to either ψ_2 or to $\psi_2 + \pi$, whichever is closer to ψ_1 [dashed curve, Fig. 1(a)]. When the two are perpendicular, $\psi_2 = \psi_1 + \pi/2$, the dashed curve collapses into the right angle and there is no continuous reorientation. In this case, when the treatment is weak, $W_a^{(2)} < W_a^{(1)}$, the resulting easy axis does not move, but the anchoring strength decreases, $W_a \to 0$. When $W_a^{(2)} > W_a^{(1)}$, the easy axis abruptly realigns from ψ_1 to $\psi_2 = \psi_1 + \pi/2$. Both the smooth rotation [5] and the threshold realignment [6] have already been observed.

In a similar way, Eq. (7) describes changes when an inhomogeneous substrate is subjected to a uniform alignment treatment $\tilde{W}_a^{(1)}$ [Fig. 1(b)]. This treatment ''hides'' the random anchoring rather than destroys it; the resulting $\tilde{W}_a(\mathbf{r})$ is the vector sum of $\tilde{W}_a^{(1)}$ and the local $\tilde{W}_a^{in}(\mathbf{r})$. This feature predicts an interesting and counterintuitive effect: the original random anchoring modified by the unidirectional treatment $\tilde{W}_a^{(1)}$ can be restored by a subsequent treatment of the same amplitude $W_a^{(2)} = W_a^{(1)}$ but of the orthogonal direction $\psi_2 = \psi_1 + \pi/2$, i.e., $\tilde{W}_a^{(2)} = -\tilde{W}_a^{(1)}$. The validity of the tensor and complex description and in particular, the compensating effect of two treatments, $\tilde{W}_a^{(2)} = -\tilde{W}_a^{(1)}$, is demonstrated experimentally below.

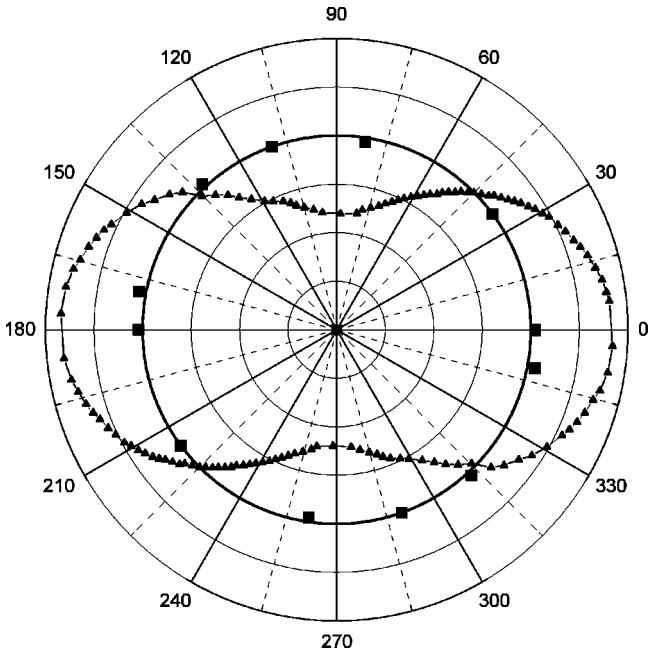

FIG. 3. Light transmittance of the cell vs the orientation of the analyzer for the nonirradiated (■) and the irradiated (▲) $\tau_1 = 60$ s cell.

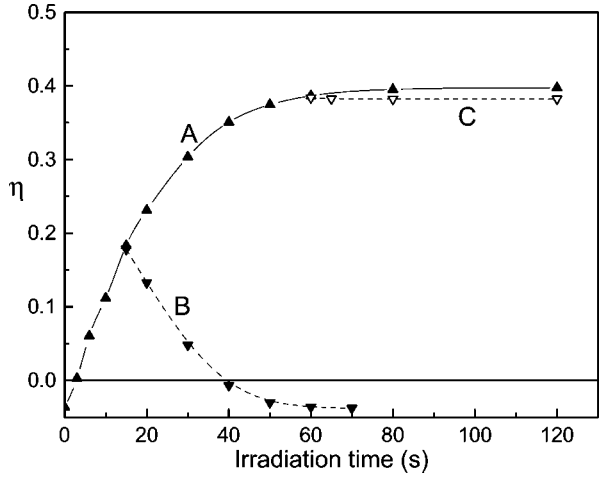

FIG. 4. The transmittance anisotropy η vs irradiation time. Curve *A* corresponds to the first irradiation with $\hat{\mathbf{e}}_{uv}^{(1)} \perp \hat{\mathbf{e}}_{rub}$. Curves *B* and *C* result from the second irradiation with $\hat{\mathbf{e}}_{uv}^{(2)} \| \hat{\mathbf{e}}_{rub}$ that follows the first irradiation of duration $\tau_1 = 15$ s and $\tau_1 = 60$ s, respectively.

Experiment

We studied the nematic LC 4,4'-n-pentylcyanobiphenyl (5CB, Merck) and the photoaligning polymer para-fluorocinnamoyl cellulose (FCCN). 5CB is placed between the reference and the FCCN substrates. The nonirradiated surface of FCCN aligns 5CB tangentially. The reference substrate is a rubbed polyimide layer that produces strong planar anchoring along the rubbing direction $\hat{\mathbf{e}}_{rub}$. The cell thickness was chosen to be large, $L = 55$ μm, to reduce the elastic torque $\sim K_{22}/L$ caused by the fact that $\hat{\mathbf{e}}_{rub}$ is generally not parallel to the local easy axis of FCCN substrate. Here K_{22} is the twist elastic constant.

Inhomogeneous anchoring at the nontreated FCCN substrate

The cell was filled with 5CB in the isotropic state (100 °C). The FCCN substrate was put in contact with a cooled surface to create a temperature gradient across the cell. The nematic phase nucleated at the FCCN surface first, and then propagated towards the reference plate. In this way, alignment of LC at FCCN was determined mainly by the anchoring properties of the FCCN surface. The alignment is inhomogeneous with characteristic size of domains $d \sim 100$ μ m; see Fig. 2(a). The reference rubbed surface faced the polarizer of the microscope, with $\hat{\mathbf{e}}_{rub}$ being parallel to the polarizer. The polarization of the transmitted light is determined by the local director orientation on the FCCN substrate (''Mauguin regime''). The total intensity of the transmitted light did not depend on the orientation of the analyzer within an error of 10%; see Fig. 3. Thus, the local azimuthal anchoring W_a^{FCCN} at the FCCN surface is random and strong enough to withstand the orienting action of the

reference rubbed substrate, $W_a^{FCCN} \gg K_{22}/L$, and the increase of elastic energy, caused by inhomogeneities $W_a^{FCCN} \gg K/d$ [7,8], where K is one of the elastic constants.

Alignment by polarized light

The cell described above was exposed to polarized uv light (Hg lamp, intensity 5 mW/cm^2) that is absorbed effectively by FCCN. The induced alignment direction $\hat{\mathbf{e}}_{uv}$ is perpendicular to the polarization of the incident light, $\mathbf{E}_{uv}$. Irradiation reorients $\hat{\mathbf{n}}$ towards $\hat{\mathbf{e}}_{uv}$ and produces macroscopic optical anisotropy of the cell; see Fig. 3. To quantify the anisotropy we use the parameter $\eta=(I_{||}-I_{\perp})/(I_{||}+I_{\perp})$, where $I_{||}$ and $I_{\perp}$ are the intensities of transmitted light measured with analyzer parallel and perpendicular to $\hat{\mathbf{e}}_{uv}$, respectively. The dependence of η on the exposure time τ (Fig. 4, curve A) corresponds to the scenario depicted in Fig. 1(b) and reveals the nonlinear effect with saturation.

Compensating effect of two orthogonal irradiations

To demonstrate the recovery of the initial inhomogeneous anchoring, the cell with nontreated substrate [Fig. 2(a)] was subjected to two subsequent uv orthogonal treatments. The first treatment with $\hat{\mathbf{e}}_{uv}^{(1)} \perp \hat{\mathbf{e}}_{rub}$ during $\tau_1=15$ s induced a 90°-twist structure in the cell [Fig. 2(b)]. The bright lines in Fig. 2(b) correspond to domain walls that separate regions with opposite rotations. The second treatment with $\hat{\mathbf{e}}_{uv}^{(2)} \perp \hat{\mathbf{e}}_{uv}^{(1)}$ (Fig. 4, curve B) exhibits the mirror behavior in comparison with curve A with respect to the value of η between the irradiations. The texture obtained after $\tau_2=45$ s when η returns to its initial value $\eta(\tau=0)$, Fig. 2(c), is essentially identical to the initial texture, Fig. 2(a), i.e., the second exposure recovers the initial pattern $\hat{\mathbf{n}}(\mathbf{r})$ in details. If $\tau_1>15$ s the recovery of $\eta(\tau=0)$ is not achievable, although $\eta(\tau)$ clearly preserves the mirror behavior (Fig. 4, curve C). The recovery of the initial texture in the saturation range for the second treatment confirms the validity of Eqs. (5) and (7), even for strong treatments.

Note in conclusion that the proposed tensor description is also a powerful tool to study the statistical properties of surface anchoring (e.g., the correlation length for easy axis, the average domain size, etc.) using the correlator $G_{\alpha\beta,\gamma\xi}(\mathbf{r}') = \langle W_{\alpha\beta}(\mathbf{r}) W_{\gamma\xi}(\mathbf{r}+\mathbf{r}') \rangle_{\mathbf{r}}$.

The authors are grateful to Igor Gerus for the synthesis of FCCN. The work was supported by the NSF STC ALCOM, Grant No. DMR89-20147 and by the Fund of the Academy of Sciences of Ukraine, Grant No. B29/13.

[1] K. Ichimura, in *Photochemical Processes in Organized Molecular Systems*, edited by K. Honda (Elsevier, Amsterdam, 1991), p. 343.

[2] T. Marusii and Yu. Reznikov, Mol. Mater. **3**, 1614 (1993).

[3] T.J. Sluckin and A. Poniewierski, in *Fluid Interfacial Phenomena*, edited by C.A. Croxton (Wiley, New York, 1985), p. 215.

[4] S.P. Palto, S.G. Yudin, C. Germain, and G. Durand, J. Phys. II **5**, 133 (1995) S.P. Palto and G. Durand, *ibid.* **5**, 963 (1995).

[5] J. Chen, D.L. Johnson, P.J. Bos, X. Wang, and J.L. West, Phys. Rev. E **54**, 1599 (1996); J.H. Kim, S. Kumar, and Sin-Doo Lee, *ibid.* **57**, 5644 (1998).

[6] A.G. Dyadyusha, T.Ya. Marusii, V.Yu. Reshetnyak, Yu.A. Reznikov, and A.I. Khizhnyak, Pis'ma Zh. Eksp. Teor. Fiz. **56**, 18 (1992) [JETP Lett. **56**, 17 (1992)].

[7] O.D. Lavrentovich and P. Palffy-Muhoray, Liq. Cryst. Today **5** (2), 5 (1995).

[8] J.-B. Fournier and P. Galatola, Phys. Rev. Lett. **82**, 4859 (1999).